SAND2019-14337C

Analysis of Laser Focusing Effect on Quantification of LII Images

Christopher R. Shaddix and Timothy C. Williams †

Combustion Research Facility
Sandia National Laboratories
Livermore, California 94550

Abstract

Laser-induced incandescence (LII) is a widely used technique for measuring soot concentrations. For flame applications LII is frequently deployed as a planar diagnostic to measure the two-dimensional soot field. However, when the laser sheet is focused, as is typical to reach the requisite laser fluence level and achieve good spatial resolution, the complex laser power dependence of the LII signal generation process can introduce a large variation in LII signal sensitivity across an LII image. In this work, this effect is quantified for the first time as a function of laser pulse fluence, using a typical planar LII excitation scheme with a clipped Gaussian YAG laser beam focused with a 1 m focal length lens. Furthermore, the cross-sectional energy distribution in the laser sheet was measured across the image plane, to relate the details of the laser sheet focal properties with the resultant LII behavior. The results show that a unique laser fluence level (referenced to the focal plane) exists whereby there is essentially no dependence of LII signal on position relative to the focal plane. However, at lower or higher fluences, the radial signals either decrease (low fluence) or increase (high fluence) rapidly with increasing distance away from the focal point. For measurements using an LII 'plateau' laser fluence level, as is usual in environments with significant optical depth (i.e. sufficiently strong soot levels), the LII signals are found to be 2.5X larger 40 mm away from the focal point. An analysis conducted by combining a previously measured LII fluence dependence for a top-hat laser profile with the laser sheet cross-sections measured in this work shows general agreement with the measured results for LII signal variation. Further, the sensitivity of LII signals at high fluences to the laser beam spatial profile, particularly away from the sheet focus, is highlighted.

Keywords: soot, laser-induced incandescence, laser, focus

† Present address: T.C. Williams and Associates, Livermore, CA.

1. Introduction

One of the advantages of using laser-induced incandescence (LII) to measure soot concentrations is its ability to instantaneously sample a two-dimensional (or even three-dimensional) soot field through planar imaging of the LII signals [e.g. 1-9]. In such applications, an optical configuration usually consisting of a plano-convex cylindrical lens and a spherical lens is used to form a planar laser sheet. The laser sheet is typically brought to a focus at the image plane to achieve the necessary laser intensity to substantially heat the soot particles and excite LII. Focusing the laser sheet also has the advantage of providing improved spatial resolution with respect to the thickness of the laser sheet.

Many laser diagnostics operate in a linear laser power excitation regime, wherein focusing the laser has no impact on the magnitude of the resultant signals, so long as the laser beam thickness is substantially less than the depth of field of the imaging optics, which is generally the case. However, LII has a highly nonlinear and complex laser excitation dependence, because of the interaction of laser absorption, convective loss, and particle mass removal on determining the instantaneous particle temperature and volume (in addition to the inherent non-linearity of the Planckian thermal emission that generates the measured LII signals) [10-12]. Furthermore, the complex temporal dynamics of LII signals means that LII signals are typically integrated over a finite time interval that includes at a minimum the entire duration of the laser excitation pulse (particularly for imaging applications, wherein a gated image intensifier is typically used), such that the dependence of LII signals on laser intensity is usually expressed as a function of the laser pulse fluence.

Figure 1 shows simulated LII laser excitation curves for signals generated at the focus of laser beams or sheets, as reported by Bladh et al. [13]. The top-hat response represents the idealized case wherein there

is no spatial variation of laser intensity, in which case the depletion of soot mass during the laser pulse for high fluence levels results in decreasing LII signals. A Gaussian sheet has a Gaussian energy distribution across the laser sheet cross-section, such that at higher laser fluence levels the decreasing signal contributions from the center of the sheet (due to soot vaporization) are almost exactly offset by additional signal contributions from LII excited in the wings of the Gaussian. A Gaussian beam, on the other hand, has expanding contributions of LII signal generation in full 2-D space as the laser fluence increases, which more than offsets the decreasing LII signal generated from the center of the beam.

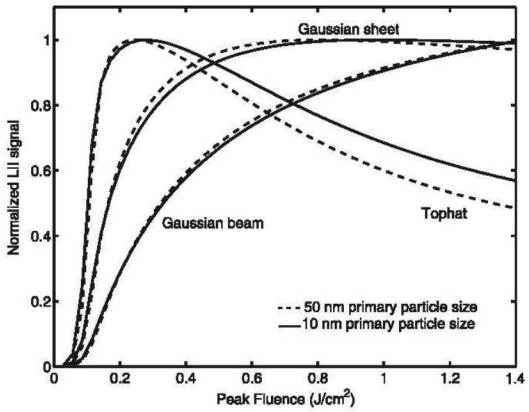

Figure 1. Simulated LII signals generated from different sized soot particles as a function of laser fluence for characteristic laser beams and laser sheets when using a 100-ns gate on the detector that opens coincident with the arrival of a 10-ns laser pulse (from Bladh et al. [13]). The laser fluence used for the Gaussian cases is the fluence in the center of the beam or sheet.

One can apply these concepts that have been historically applied to interpret the LII laser fluence dependence *at the laser focus* to understand what happens as a laser sheet expands away from the focal point. Because the LII signal generation for a Gaussian sheet is relatively constant with fluence level, once a suitable fluence level has been reached, if the fluence at the focal point is above this critical fluence, moving away from the focal point will result in *greater* LII signal, as a broader region of soot will be heated by the laser pulse and therefore contributing to the incandescence signal. Indeed, Shaddix and

Smyth [14] first reported this phenomenon, as shown in Fig. 2, when imaging LII excited by a Gaussian beam. Their study revealed a 20% increase in LII signal just 10 mm away from the laser focal point and larger increases in LII signals for distances further away from the laser beam focus. Despite the apparent need for a significant signal correction across an LII image plane, subsequent LII imaging studies have neither investigated nor accounted for this phenomenon in their own measurements, perhaps under the belief that by forming a laser sheet with a longer focal length lens that it would become insignificant.

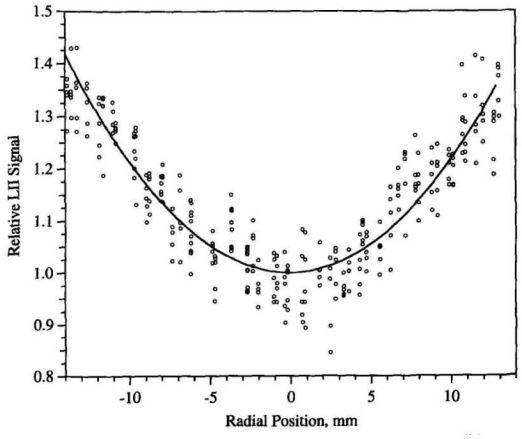

Figure 2. Transverse LII signal strength reported by Shaddix and Smyth [14] when imaging LII signals along a Gaussian laser beam focused with a 300 mm focal length lens.

The study reported here is an attempt to fully understand and quantify the laser focusing effect on LII planar imaging. To accomplish this, a 1064 nm Gaussian ns laser excitation source and a 1 m focal length spherical lens is used, as is commonly employed for LII planar imaging. The laser fluence is varied and the LII signal intensity is measured for a range of distances on either side of the laser sheet focus. Further, to develop a concrete understanding of how the details of the laser focusing properties affect the LII signal, the laser sheet cross-section has been imaged at discrete locations as it approaches and recedes from the focal point. These laser sheet cross-sections are used, together with a previously reported measurement of the LII laser fluence dependence generated from a top-hat laser beam, to calculate the effect of laser sheet defocusing on the planar LII signals, in comparison with the actual LII signal measurements.

2. Experimental Methods

Laser-induced incandescence was excited using the 1064 nm output from an injection-seeded 10-Hz Nd:YAG laser with a pulse duration of approximately 9 ns that was subsequently expanded into a two-dimensional beam and mildly focused above a burner, as shown in Fig. 3. To vary laser power without otherwise perturbing the laser characteristics, a half-wave plate was used, in conjunction with a glan laser polarizer. An iris was placed in a relay imaging system downstream of the polarizer to provide mild clipping of the laser beam, reducing its intensity by approximately 50%. Note that a top-hat laser beam profile was not employed in this study (as indeed it rarely is for LII imaging applications) because formation of a top-hat profile requires rejecting the vast majority of the initial laser beam intensity, thereby restricting the range of laser fluences that can be investigated with laser sheet excitation of LII.

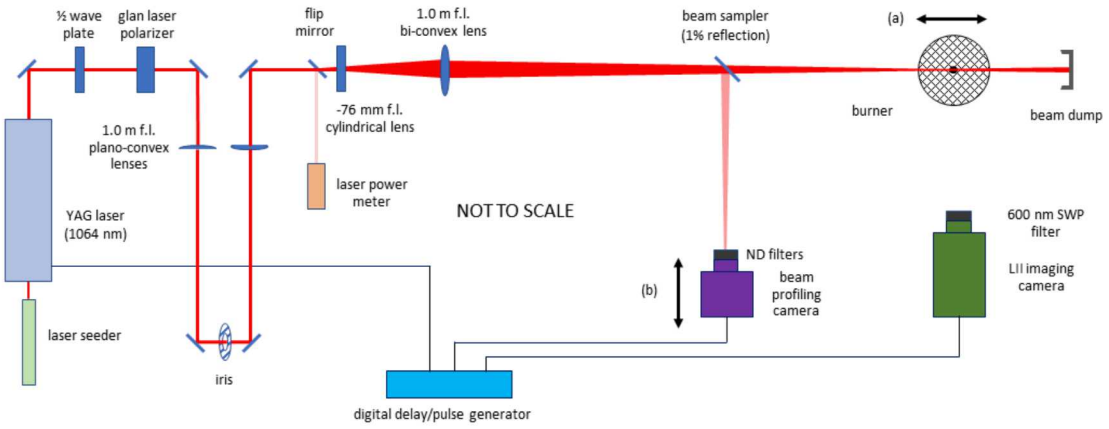

Figure 3. Schematic of the experimental layout. Motion "(a)" indicates burner translation that was used to move a soot feature in a flame across the LII image plane, whereas motion "(b)" indicates how laser sheet profiling measurements were made along the beam path in the vicinity of the focal point.

LII signals were collected using a Princeton Instruments fast-gating PIMAX CCD camera, with 512 x 512 pixels and a HQf GEN III intensifier. A 600 nm short-pass filter was placed in front of the

camera, to distinguish LII signals from flame luminosity, and a 100 ns gate was employed on the intensifier, opening as the laser pulse arrived in the probe volume.

A non-premixed jet flame burner was used to establish both laminar and turbulent oxy-fuel flames that contained soot. The burner consists of coannular fuel and oxidizer tubes surrounded by a well-conditioned air stream to provide a stable flame environment and establish definitive boundary conditions. It has been previously described in detail in the literature [15]. Flow rates of 5.00 slpm (referenced to 293 K) CH_4 and 7.50 slpm O_2 were used in the investigated laminar flame, and the measurements were performed at a height of 102 mm. This height was chosen because it is well downstream of the soot inception zone (so the soot should be fairly well carbonized) and the soot field at this height formed approximately vertical profiles on either side of the burner centerline, allowing the LII signal response across the image plane to be measured by translating the burner (and thus these vertical profiles) to the right and left. The LII imaging camera was maintained in a fixed position, as it had a field of view of 90 mm width at the flame, allowing ample side-to-side translation of the burner while still measuring the LII signals. At each transverse flame measurement position, 200 images were captured. Within each image, the peak LII signal corresponding to the annular soot layer was identified and then averaged across the ensemble of images (thereby correcting for any slight flame wobble from image to image).

Because the motivation for investigating the transverse dependence of LII signals is for making measurements in turbulent flames with a broad flame brush, turbulent methane and ethylene oxy-fuel flames were also investigated, though only with respect to the fluence dependence of LII signals at the laser sheet focus. The investigated turbulent methane flame was the same flame from a previously reported study [15] with 50% O_2 in N_2 in the oxidizer flow. LII fluence dependence was determined along the center of the flame at a height of 290 mm, corresponding to the location of the peak mean soot volume fraction. The turbulent ethylene flame used the same nominal flow rates as the turbulent methane flame and had a peak mean soot volume fraction at a height of 350 mm, which is where the LII fluence

dependence was measured. For both turbulent flames, 20,000 LII images were collected at each laser power level and averaged, to account for the strong intermittency of soot in these flames.

To image the laser sheet energy profile as it approached and receded from its focal point, a WinCamD CMOS laser beam-profiling camera was placed on a horizontal translation stage downstream of a beam sampler, which reflected 1% of the incident laser sheet. A combination of an ND4 and an ND1 filter was placed in front of the camera to further reduce the laser power to an acceptable level. 64 laser shots were averaged at each location. The camera has an 11.3 mm x 11.3 mm square sensor, divided into 2048 pixels in each direction (5.5 μm pixel dimension). To interrogate the full height of the laser sheet, the camera was mounted on a lab jack and was translated to collect a series of vertical images, which were subsequently combined.

3. Results

3.1 LII signal measurements

Figure 4 shows the measured variation in LII signal for various laser powers at the laser sheet focus, whose approximate location was determined by using burn paper. Laser power is used as the abscissa in this figure because the laser power (or laser pulse energy, which in this case is equal to the power divided by 10) is a well-defined entity, as opposed to laser fluence, which requires an estimate of laser sheet width (in fact, the laser sheet fluence will be analyzed in depth later). Further, when comparing signals at the laser sheet focus with signals away from the focus, the fluence level varies with spatial location, whereas the laser power does not. There are several things to note in Fig. 4. The first is that the LII signals decrease with increasing laser fluence once an initial signal peak is reached, consistent with the theoretical modeling shown in Fig. 1. At laser powers well past the initial LII peak, the signals 'bottom out', after a decrease of approximately 30% from the peak LII signal, and start to increase again. This trough region is the best region to operate a laser to achieve LII signals that are relatively insensitive to laser power (i.e. to achieve

LII ‘plateau’ signal dependence), if desired. For example, use of an initial 1.5 W laser power will allow 40% laser absorption in a flame (giving a flame exit laser power of 0.9 W) without substantially affecting the generated LII signals. Fig. 4 also shows that the LII signal variation with laser power is effectively the same whether one is interrogating a laminar or turbulent flame and is generally independent of the fuel used in the flame.

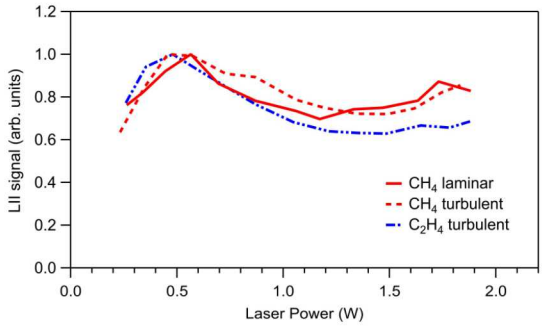

Figure 4. Measured LII signal variation at the laser sheet focus as a function of laser power.

Figure 5 shows the measured LII signal variation in the laminar methane flame as a function of both laser power and position relative to the nominal laser sheet focus. For low laser powers, before the initial peak in LII signal, moving away from the laser sheet focus results in lower LII signals, because the local laser fluence is lower, such that the soot particles are heated less and emit less thermal radiation. At higher laser powers, when moving both upstream and downstream from the laser focus, the laser power at which the LII signal reaches a peak increases, and the LII signals themselves also increase. This can be explained according to the interaction of two phenomena: (a) the soot in the middle of the beam is experiencing less evaporation as one moves away from the laser sheet focus and therefore is emitting a stronger LII signal relative to the sheet focus (i.e. there is less ‘signal bleaching’), and (b) the physical expansion of the laser sheet away from the laser sheet focus results in excitation of a thicker segment of soot. In comparing the two sides of Fig. 5, the same general trends are evident upstream and downstream of the laser sheet focus.

Also, the LII signal dependence for the position denoted '-10 mm' is nearly identical to that at the nominal laser sheet focus, suggesting that the true laser sheet focus lies somewhere between -10 mm and 0 mm. With that observation, the differences in the '-20 mm' and '+20 mm' profiles and the '-30 mm' and '+30 mm' profiles may, at least in part, be attributed to differences in their locations relative to the true laser sheet focus.

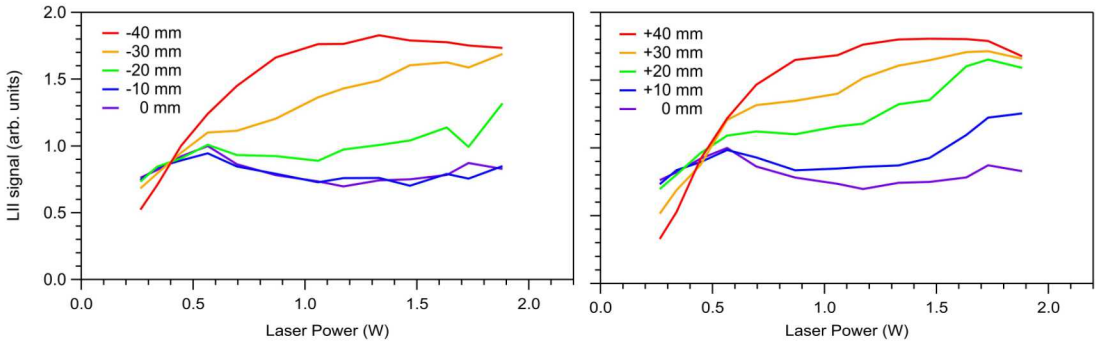

Figure 5. Measured LII signal variation for different transverse positions relative to the nominal laser sheet focus as a function of laser power. The plot to the left shows positions upstream of the laser sheet focus, while the plot to the right shows positions downstream of the laser sheet focus.

For a given laser power, one can use the data shown in Fig. 5 to compute the variation in LII signal with position relative to the nominal laser sheet focus, as shown in Fig. 6. As is evident in this figure, soot that is imaged 40 mm away from the laser sheet focus (i.e. 40 mm away from the flame centerline, in typical LII setups) will have up to **2.5x higher LII signal** (i.e. 2.5x higher indicated soot volume fraction) than soot imaged on the flame centerline, depending on the laser power that is used. Clearly, this phenomenon can be a major factor in the quantification of LII images, particularly in turbulent flames, wherein the soot-containing regions often extend 40 mm from the flame centerline. Conversely, if the laser shot-to-shot laser power is stable and the interrogated flame environment is optically thin, the results shown in Fig. 6 motivate the use of a laser power just slightly less than that corresponding to the initial peak of LII signal at the focus (i.e. approx. 450 mW in the current example), because at this laser power

the LII signals are independent of position relative to focus. This distinctive condition is evident in Fig. 5 as the laser power wherein the LII signal curves cross one-another.

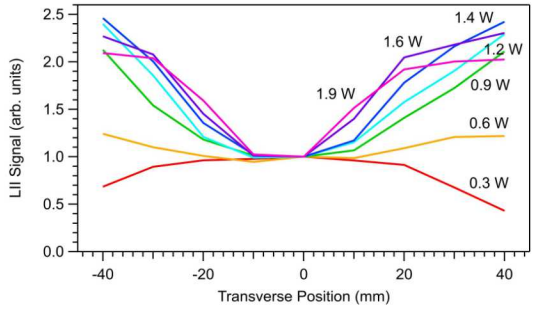

Figure 6. Measured LII signals as a function of transverse position relative to the nominal laser sheet focus for different laser powers.

For LII imaging in flames with significant laser absorption, it is important to excite the LII with a laser fluence that is somewhat greater than the threshold fluence associated with peak LII signals at the laser focus, because with threshold fluence excitation any absorption of the beam would result in a rapid decrease in LII signals. Fig. 6 shows that for laser excitation intensities between 0.9 and 1.5 W, the LII intensity measured at different positions relative to the laser focus is relatively constant, meaning that an average transverse correction to the measured LII signal can be applied with reasonable accuracy, as indicated in Fig. 7. Whereas Figs. 6-7 show similar LII signal variation upstream and downstream of the laser sheet focus, there are somewhat lower signals and greater variation with position in the signals downstream of the focus, presumably reflecting minor differences in the spatial characteristics of the laser sheet before and after its focus, as will be explored in the next section.

3.2 Laser sheet cross-sections and computed LII signals

Figure 8 shows the laser sheet cross-sectional energy distributions upstream and downstream of the nominal laser sheet focus. Whereas the central peaks show clear Gaussian character, there are uneven wing contributions which become increasingly apparent away from the focal plane. Minor differences are

also apparent in the profiles approaching and receding from the focal plane. The $1/e^2$ cross-sectional diameter of the sheet at the focal plane is measured to be 180 μm. Using this definition of beam diameter, together with the 11.8 cm laser sheet height, the fluence at the laser power (0.55 W) that generated the initial peak in LII signal at the laser sheet focus is 0.26 J/cm^2.

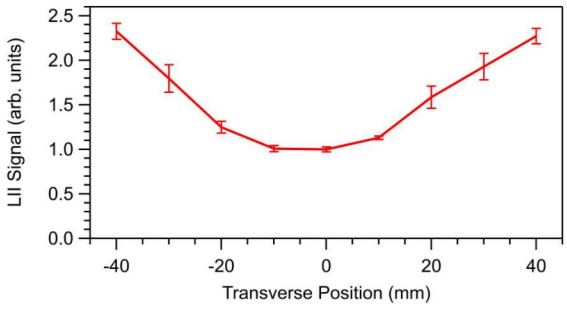

Figure 7. Average LII signal variation as a function of transverse position relative to the nominal laser sheet focus for laser powers between 0.9 and 1.5 W. The error bars indicate the range of variation in signals over these laser powers.

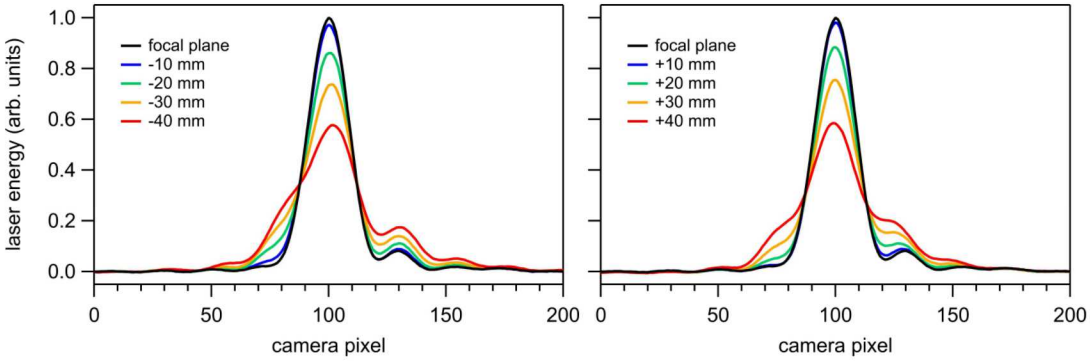

Figure 8. Measured laser sheet energy distributions at mid-height of the sheet for different axial positions relative to the nominal laser focus. Note that the laser focal position relative to the beam profiling camera was estimated, such that the nominal focal point here is likely slightly different than that indicated for LII imaging.

To relate the measured laser sheet cross-sections to LII signal generation, information is needed regarding the generation of LII signals as a function of *local* laser fluence at a given position in the laser sheet. Witze et al. [16] performed detailed measurements of both time-resolved and time-integrated LII

signals when exciting LII with a top-hat laser profile over a broad range of laser powers. A time-integrated profile from Witze is shown in Fig. 9, together with the best-fit analytical function that could be readily identified, which utilized a combination of two exponential functions.

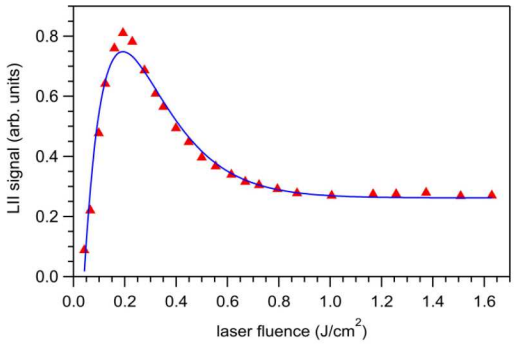

Figure 9. Measured LII signal dependence in a top-hat laser beam for a 50 ns prompt gate (symbols), from Witze et al. [16], and analytical function fit to the data (line).

LII signal generation for the laser sheet used in the current study was computed by utilizing the analytical fit to Witze's data to compute LII signal contributions from each location within the laser sheet cross-sectional profile and then integrating across the sheet. Of course, there are differences in the way the LII signals were generated and measured in the current study in comparison to the Witze measurements, including the timing gate detection window and spectral range of LII detection. Most importantly, though, Witze used a 532 nm YAG beam to excite the LII. To correct for the lower soot absorptivity of the 1064 nm laser used in the current study, the Witze fluence levels were multiplied by 2 for application to the 1064 nm beam, reflecting the approximately $1/\lambda$ dependence of mature soot absorptivity over these wavelengths [17]. Figure 10 shows the computed LII signals as a function of laser power and position relative to the laser sheet focus. Results are shown both with the measured cross-sectional beam profiles and with the Gaussian fits to the cross-sectional profiles, to demonstrate the sensitivity of the LII signal strength at high laser powers, away from the laser focus, to the details of the laser sheet cross-sectional energy distribution. When comparing the computed results in Fig. 10 to the

corresponding measured LII signals in Fig. 5, it is apparent that the overall trends in the experimental data are well predicted, though the laser power at which the signal at the laser sheet focus reaches a peak is overpredicted, as is the laser power at which the different profiles cross one-another. The results for the Gaussian fits confirm that the trend of large LII signal variation with transverse position is a general phenomenon, not limited to the particulars of the clipped Gaussian sheet experimentally explored in this work.

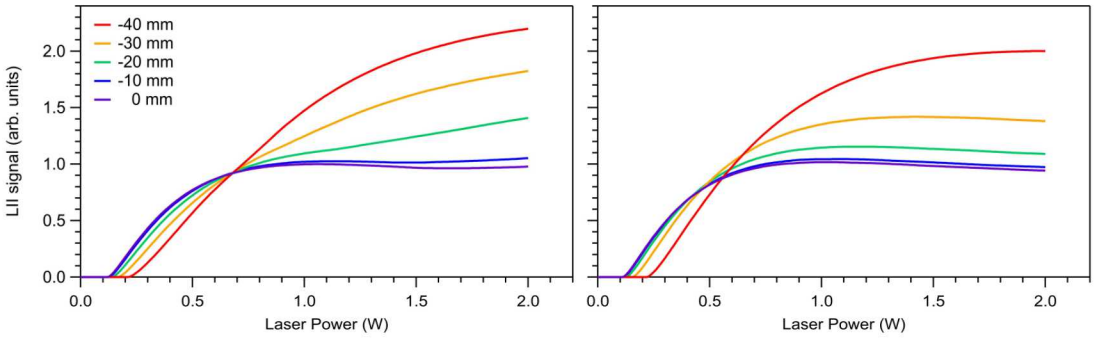

Figure 10. Calculated LII signals as a function of laser power for different distances from the laser sheet focus. The plot on the left shows the results using the measured cross-sectional energy distribution in the laser sheet whereas the plot on the right was computed using Gaussian fits to the actual spatial distribution. Results are shown upstream of the laser sheet focus; similar results were found downstream of the focus.

4. Conclusions

This work has investigated the variation in LII signals as a function of laser sheet position relative to its focal point, using a standard focusing lens with a 1 m focal length. For laser energies exceeding the 'threshold' LII fluence wherein soot particle vaporization becomes important, a strong sensitivity is found in LII signals as one moves away from the laser focus, resulting in a factor of 2.5 variation in apparently soot concentrations when imaging soot 40 mm away from the burner centerline. Conversely, for a laser fluence slightly below the threshold fluence, LII signals remain constant for positions up to +/- 40 mm

from the laser sheet focus. Thus, this near-threshold fluence is recommended for use when performing LII imaging measurements in lightly sooting flames. On the other hand, for flames in which significant laser absorption occurs, one can use a high fluence that yields a consistent 'plateau' fluence dependence over a range of positions relative to the focal point and correct for the apparent transverse dependence in LII signals on the imaging camera. However, calculation of LII signal generation using cross-sectional energy distributional data demonstrates that signals away from the focus are sensitive to minor variations in laser beam shape at high laser powers, such that it is important that the laser operate consistently if one is to conduct LII measurements in this regime.

Acknowledgments

Support for this research was provided by Sandia National Laboratories' Laboratory Directed Research and Development program. Sandia National Laboratories is a multimission laboratory managed and operated by National Technology and Engineering Solutions of Sandia, LLC., a wholly owned subsidiary of Honeywell International, Inc., for the U.S. Department of Energy's National Nuclear Security Administration under contract DE-NA-0003525. The views expressed in the article do not necessarily represent the views of the U.S. Department of Energy or the United States Government.

References

[1] J.E. Dec, A.O. zur Loye, D.L. Siebers, D.L., Soot distribution in a diesel engine using 2-D laser-induced incandescence imaging. SAE Paper 910224, 1991.

[2] F. Cignoli, S. Benecchi, G. Zizak, Time-delayed detection of laser-induced incandescence for the two-dimensional visualization of soot in flames, Appl. Optics 33 (1994) 5778–5782.

[3] T. Ni, J.A. Pinson, S. Gupta, R.J. Santoro, Two-dimensional imaging of soot volume fraction by the use of laser-induced incandescence, Appl. Optics 34 (1995) 7083–7091.

[4] R.L. Vander Wal, D.L. Dietrich, Laser-induced incandescence applied to droplet combustion, Appl. Optics 34 (1995) 1103–1107.

[5] H. Geitlinger, Th. Streibel, R. Suntz, H. Bockhorn, Two-dimensional imaging of soot volume fractions, particle number densities and particle radii in laminar and turbulent diffusion flames. Proc. Combust. Inst. 27 (1998) 1613–21.

[6] C.R. Shaddix, T.C. Williams, L.G. Blevins, R.W. Schefer, Flame structure of steady and pulsed sooting inverse jet diffusion flames, Proc. Combust. Inst. 30 (2005) 1501–1508.

[7] T.R. Meyer, S. Roy, V.M. Belovich, E. Corporan, J.R. Gord, Simultaneous planar laser-induced incandescence, OH planar laser-induced fluorescence, and droplet Mie scattering in swirl-stabilized spray flames, Appl. Optics 44 (2005) 445–454.

[8] S.-Y. Lee, S.R. Turns, R.J. Santoro, Measurements of soot, OH, and PAH concentrations in turbulent ethylene/air jet flames, Combust. Flame 156 (2009) 2264–2275.

[9] J.B. Michael, P. Venkateswaran, C.R. Shaddix, T.R. Meyer, Effects of repetitive pulsing on multi-kHz planar laser-induced incandescence imaging in laminar and turbulent flames, Appl. Optics 54 (2015) 3331–3344.

[10] R. J. Santoro, C.R. Shaddix, Laser-Induced Incandescence, in: K. Kohse-Höinghaus, J.B. Jeffries (Eds.), Applied Combustion Diagnostics, Taylor and Francis, New York, 2002, pp. 252–286.

[11] C. Schulz, B.F. Kock, M. Hofmann, H. Michelsen, S. Will, B. Bougie, R. Suntz, G. Smallwood, Laser-induced incandescence: recent trends and current questions, Appl. Phys. B 83 (2006) 333–354.

[12] H. Michelsen, C. Schulz, G.J. Smallwood, S. Will, Laser-induced incandescence: Particulate diagnostics for combustion, atmospheric, and industrial applications, Prog. Energy Combust. Sci. 51 (2015) 2-48.

[13] H. Bladh, P.-E. Bengtsson, Characteristics of laser-induced incandescence from soot in studies of a time-dependent heat- and mass-transfer model, Appl. Phys. B 78 (2004) 241–248.

[14] C.R. Shaddix, K.C. Smyth, Laser-induced incandescence measurements of soot production in steady and flickering methane, propane, and ethylene diffusion flames, Combust. Flame 107 (1996) 418–452.

[15] C.R. Shaddix, T.C. Williams, The effect of oxygen enrichment on soot formation and thermal radiation in turbulent, non-premixed methane flames, Proc. Combust. Inst. 36 (2017) 4051–4059.

[16] P.O. Witze, S. Hochgreb, D. Kayes, H.A. Michelsen, C.R. Shaddix, Time-resolved laser-induced incandescence and laser elastic-scattering measurements in a propane diffusion flame, Appl. Optics 40 (2001) 2443-2452.

[17] J. Simonsson, N.-E. Olofsson, S. Torok, P.-E. Bengtsson, H. Bladh, Wavelength dependence of extinction in sooting flat premixed flames in the visible and near-infrared regimes, Appl. Phys. B 119 (2015) 657-667.